Structural Eng./Earthquake Eng., JSCE, Vol. 19, No. 2, 131s—140s, 2002 October
(J. Struct. Mech. Earthquake Eng., JSCE, No. 717/ I —61)

A SEISMIC RISK ASSESSMENT PROCEDURE FOR GRAVITY TYPE QUAY WALLS

Koji ICHII[1]

[1]Member of JSCE, M.Eng., Researcher, Port and Airport Research Institute
(Nagase 3-1-1, Yokosuka 239-0826, Japan)

A seismic risk assessment procedure based on the fragility curve concept is proposed in this paper. First, damage criteria for gravity type quay walls in terms of normalized seaward displacement are proposed considering the restoration cost. Second, a procedure to generate the fragility curve for each damage level using Monte Carlo simulation is proposed. Third, the fragility curves are utilized for the risk assessment of a quay wall under certain conditions based on the result of seismic hazard analysis. Finally, the proposed risk assessment procedure is examined with a case history from the 2000 Tottori-ken seibu earthquake.

Key Words: *quay wall, deformation, seismic risk, seismic performance, fragility curves*

1. INTRODUCTION

As engineering tools for the performance based seismic design, various kinds of numerical techniques have been developed for port structures. The applicability of these methods for gravity type quay walls has been verified with case histories. One of the most classical methods is the Newmark type sliding block model[1), 2)]. And one of the most advanced methods is the effective stress based FEM or FDM analysis[3), 4)]. Furthermore, an empirical approach and a simple charts approach based on a parametric study have been also proposed[5), 6)]. Thus, the designer of a gravity type quay wall can choose the most appropriate numerical technique based on the available resources such as cost, time, and amount and accuracy of input information.

Although these numerical methods are deterministic procedures, the future strong ground motion level is known only probabilistically. Therefore, it is difficult to evaluate the benefit of seismic retrofit such as liquefaction countermeasures properly. No matter how the designer wants to install the liquefaction countermeasures in the foundation of a quay wall, it is impossible to check the cost/benefit balance.

To overcome this problem, a seismic risk assessment procedure based on the fragility curve concept is proposed in this paper. Here, the risk is defined as the annual expectation of loss (*AEL*), given as the product of probability and loss as follows[7)].

$$AEL = \int_0^\infty P_h(x) \sum_j \left\{ P_f(c_j|x) \cdot c_j \right\} dx \qquad (1)$$

Where, $P_h(x)$ is the hazard (annual probability of occurrences for strong ground motion level of x); $P_f(c_j|x)$ is the fragility defined as the conditional probability of occurrence of j-th damage level for strong ground motion level of x; and c_j is the magnitude of loss for the j-th damage level. It should be noted here that $P_f(c_j|x) \cdot c_j$ is defined as the fragility instead of $P_f(c_j|x)$ in some paper[7)].

Once the risk to the quay wall is estimated, risk reduction using seismic performance improvement (seismic retrofit) can be regarded as the benefit, and hence, the designer can discuss the cost/benefit balance of the improvement. Although the risk can be defined in other ways, AEL is focused as the basis of risk management from the viewpoint that seismic risk should be managed not only by reduction with retrofit but also by transferring with insurance. AEL might be a useful index for operating earthquake disaster insurance in future.

Table 1 Damage criteria for gravity type quay walls[8)]

Level of damage		Degree I	Degree II	Degree III	Degree IV
Gravity wall	Normalized residual horizontal Displacement	Less than 1.5%	1.5～5%	5～10%	Larger than 10%
	Residual tilting towards the sea	Less than 3°	3～5°	5～8°	Larger than 8°
Apron	Differential settlement on apron	Less than 0.03～0.1m	N/A	N/A	N/A
	Differential settlement between apron and non-apron areas	Less than 0.3～0.7m	N/A	N/A	N/A
	Residual tilting towards the sea	Less than 2～3°	N/A	N/A	N/A

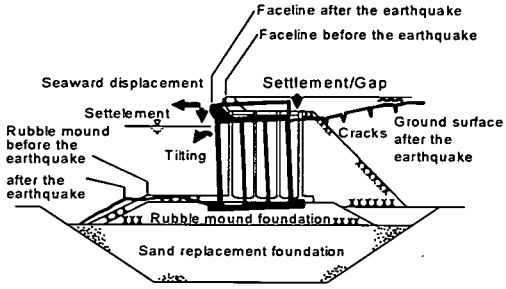

Fig.1 The typical failure mode of gravity type quay wall due to the earthquake

2. SEISMIC DAMAGE CRITERIA

Gravity type quay walls are made of a concrete caisson or other retaining structure placed on a foundation, sustaining earth pressures from backfill soil behind the wall. For this type of quay wall, the typical failure mode due to an earthquake is a seaward displacement and tilting of the walls as shown in **Fig.1**. Thus, the damage criteria can be defined by many factors, such as seaward displacement, settlement, tilting, etc. **Table 1** is an example of damage criteria for gravity type quay walls[8)]. To consider the loss, restoration case histories and their costs are examined. The typical restoration patterns after the Kobe Port disaster in 1995 are summarized in **Fig.2**[9)]. The earth pressure reduction method is used only when the deformation of the wall is relatively small and the structural integrity of the caisson is maintained. The re-installation method is for the case that the deformation of the wall is relatively large and sufficient reduction of earth pressure is difficult. The detached structure method is adopted when there is no restriction in the water space in front of the new structure. Thus, the choice of restoration method depends on not only the damage level but also many factors such as space restrictions.

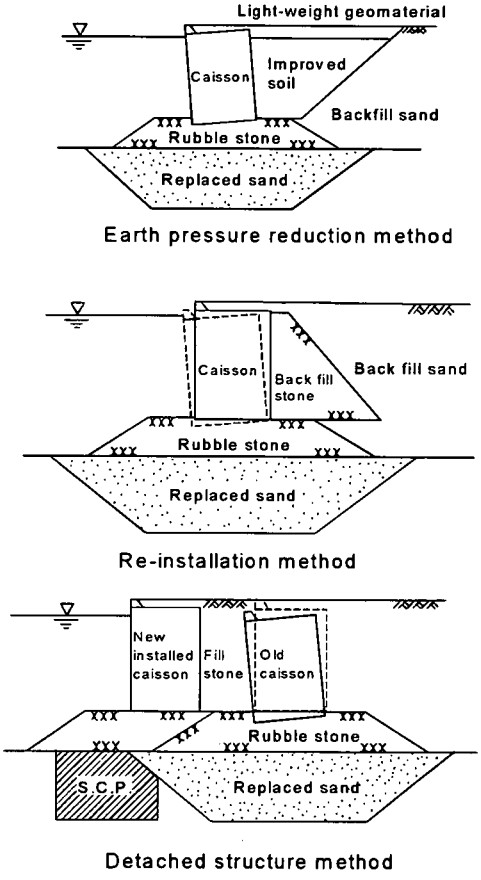

Fig.2 The typical restoration pattern for gravity type quay walls[9)]

The 36 case histories with restoration cost in Kobe Port after the 1995 Hyogoken-nanbu earthquake and Kushiro Port after the 1993 Kushiro-oki

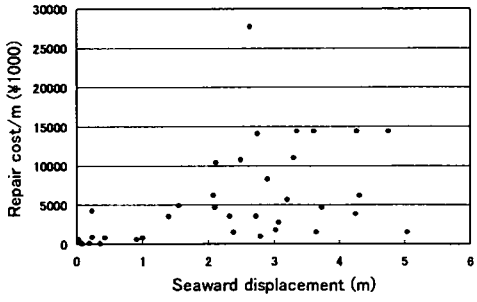

(a) Compared to seaward displacement

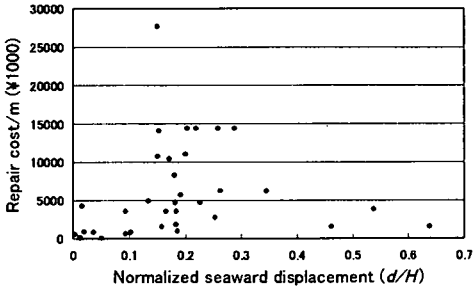

(b) Compared to normalized seaward displacement

Fig.3 Case histories of restoration cost for unit length

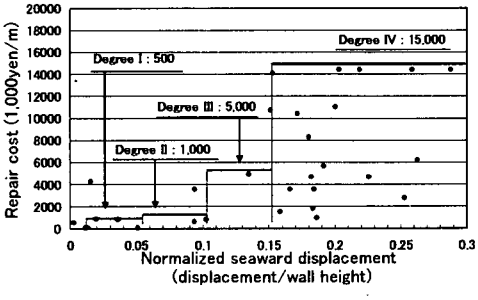

Fig.4 Proposed damage criteria based on restoration cost

earthquake are examined[10), 11)]. **Fig.3** shows the rough estimation of restoration cost per unit length (per meter along the face line) against the seaward displacement and the normalized seaward displacement at the top of the wall (seaward displacement divided by the wall height). Since the restoration cost depends on many factors such as restoration method, quay wall scale, etc, no unique relation between damage level and restoration cost is identified in **Fig.3**. However, as a rough estimation, the author defines four levels of damage criteria as shown in **Fig.4** and **Table 2**, considering the proposed criteria

Table 2 Proposed damage criteria and its loss

Damage level	Normalized seaward displacement (d/H)	Loss (1000yen/m)
Degree I	1.5～5%	500
Degree II	5～10%	1,000
Degree III	10～15%	5,000
Degree IV	Larger than 15%	15,000

shown in **Table 1**. It should be noted here that the restoration costs in **Fig.3** are a very rough estimation and sometimes include retrofit costs such as liquefaction countermeasures after the earthquake. However, these costs do not include indirect loss such as the economic impact on society. Since the cases for $d/H > 0.3$ or cost > 20,000 are very few, only the cases for $d/H < 0.3$ and cost < 20,000 are considered in **Fig.4**. Although these points are left for future research, the author moves forward to propose a risk assessment procedure.

3. FRAGILITY CURVE GENERATION USING MONTE CARLO SIMULATION

The fragility curve is a widely practiced approach to evaluate the seismic vulnerability of structures in terms of probability[12)]. In the fragility curve approach, it is assumed that the curve is expressed in the form of two parameter lognormal distribution functions. Thus, the estimation of the two parameters (median and log-standard deviation) is carried out with the maximum likelihood method. The likelihood function for the present purpose is expressed as follows.

$$L = \prod_{i=1}^{N} \left[F(a_i)\right]^{x_i} \left[1 - F(a_i)\right]^{1-x_i} \qquad (2)$$

Where $F(\cdot)$ represents the conditional probability of occurrence for the specific state of damage; a_i is the peak input acceleration, commonly referred to as PGA, however, the peak basement acceleration in terms of rock outcrop motion (2E) is used in this paper; x_i =1 or 0 for the case that the quay wall sustains the state of damage or not, respectively, under the current input excitation; and N is the total number of case histories. Under the current lognormal assumption, $F(a)$ takes the following analytical form:

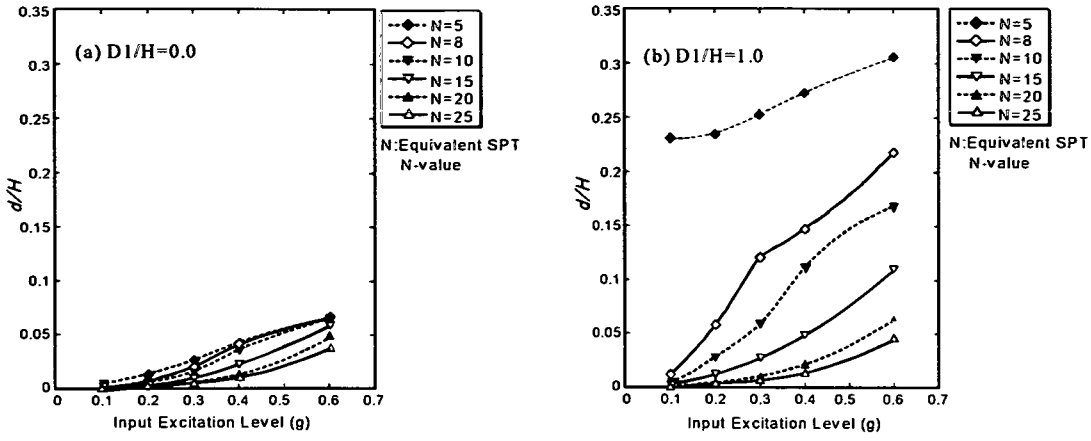

Fig.5 An example of the seismic performance evaluation charts (for *W/H*=0.9)

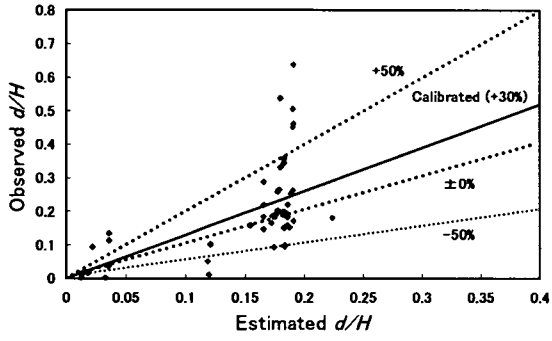

Fig.6 Applicability verification results of the seismic performance evaluation charts

$$F(a) = \Phi\left[\ln(a/c)\Big/\zeta\right] \tag{3}$$

in which a represents the peak acceleration, and c and ζ in (3) are computed as c_e and ζ_e satisfying the following equations to maximize $\ln L$ and hence L:

$$\frac{d\ln L}{dc} = \frac{d\ln L}{d\zeta} = 0 \tag{4}$$

Since this computation can be carried out by a straightforward algorithm, the only remaining problem is that of how to collect or generate enough case histories considering all of the parameters that can be varied.

Instead of gathering actual case histories, Monte Carlo simulation method is adopted in this paper to generate case histories. **Fig.5** is an example of simple seismic performance evaluation charts for gravity type quay walls developed by the author[6]. In these charts, the evaluation of seismic performance is done using the aspect ratio of the caisson wall (*W/H*), the normalized depth of the sand deposit below the wall (*D1/H*) and the equivalent SPT N values below and behind the caisson (*N65*). This chart method is verified with 55 case histories in Kobe Port and Kushiro Port as shown in **Fig.6**. Though some cases yield more than twice the observed values and some other cases yield less than half of the observed values, there is good agreement in general.

Based on linear regression analysis on these results for the condition that the regression curve go through the origin, a correction factor of $\hat{b}_1 = 1.2997$ and standard error of $\hat{\sigma} = 0.10914$ for error ε are obtained for the following equation.

$$d/H_{\_observed} = b_1\left(d/H_{\_estimated}\right) + \varepsilon \tag{5}$$

However, the error distribution for equation (5) is uniform regardless of the calibrated damage level. Therefore, the variability of Monte Carlo simulation results might be relatively large for the small damage level. Therefore, another equation (5)' is also proposed as follows.

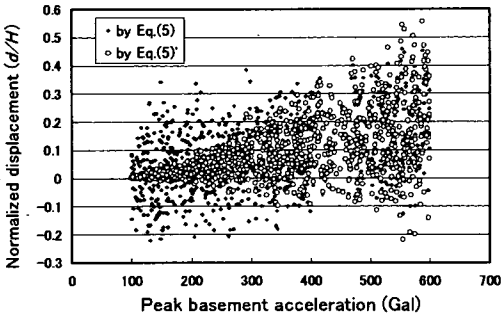

Fig.7 Examples of Monte Carlo simulation results

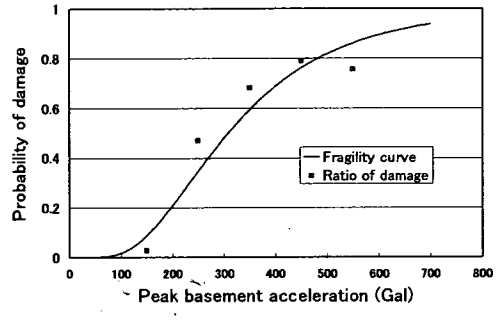

Fig.8 An example of fragility curve generation

$$d/H_{\_observed} = (b_1 + \varepsilon')(d/H_{\_estimated}) \qquad (5)'$$

Where, the correction factor $\hat{b}_1 = 1.2997$ is the same as before, but the standard error of $\hat{\sigma} = 1.05176$ is different.

Using these equations, Monte Carlo simulation of 1000 samples was carried out with the following procedure for a specific condition.

1) Produce 1000 samples of input acceleration level in the range of 100 to 600 Gal with a uniform distribution.
2) Obtain estimates of the damage for each input acceleration level for a specific condition based on the charts. Since the original numerical parametric study for charts was conducted on discrete values of 100, 200, 300, 400 and 600 Gal, the estimation is given by linear interpolation with these values.
3) Apply equation (5) or (5)' with a random error distribution to the each estimation.
4) Finally, obtain 1000 case histories of damage considering the overall variability in a specific condition.

Fig.7 shows an example of 1000 case histories generated by Monte Carlo simulation with both equation (5) and (5)' for the input of *W/H*=0.9, *D1/H*=0.5, *N65*=10. Using equation (5), the generated results are scattered over a wide range regardless of input acceleration level. However, using equation (5)', the scatter of the generated results is much lower and the relationship between the results and the input acceleration level can be recognized. Thus, the procedure using equation (5)' can be regarded as the better procedure for the risk assessment than the procedure with equation (5), implying the importance of the choice of regression equation. It should be noted here that if the generated displacement is negative, it is regarded as zero damage for simplicity.

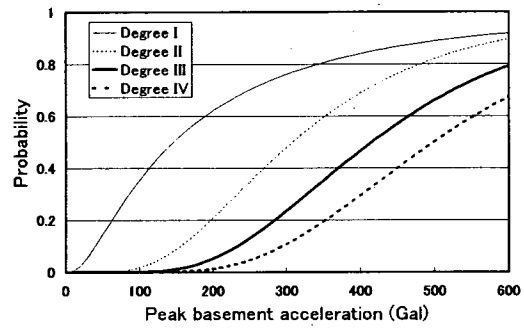

Fig.9 Examples of generated fragility curves

An example of fragility curve calibration is shown in **Fig.8**, which is for the specific condition of *W/H*=0.9, *D1/H*=0.5, *N65*=10 and for the damage degree II. Since generated cases are too numerous, the damage ratios of generated cases for each 100Gal are shown in this figure as a reference. Thus, the calibrated fragility curve shows a good agreement with the generated case histories. As an example, the fragility curves for this condition are shown in **Fig.9**. As a summary the calibrated parameters for the each line in the evaluation charts are shown in **Table 3**. Since the generated case histories scattered much, the conditional probability of damage in fragility curve for low-level input motion were quite large for the strict damage criterion case (Degree I) or extreme weak foundation case (*N65*=5). Thus, applicability of proposed fragility curves for such extreme cases should be examined in future research. It also should be noted here that the calibrated fragility curves do not give the conditional occurrence probability of the damage level discussed in equation (1). For example, the conditional probability of occurrence for degree II can be evaluated by subtract-

Table 3 Calibrated parameters of fragility curves

Equivalent SPT N values	Aspect ratio (*W/H*)	Normalized thickness of sand deposit (*D1/H*)	Degree I		Degree II		Degree III		Degree IV	
			c	ζ	c	ζ	c	ζ	c	ζ
5	0.90	0.00	160.1	1.12	414.8	0.50	615.6	0.38	689.7	0.25
8	0.90	0.00	246.3	0.65	438.5	0.40	611.9	0.33	663.7	0.19
10	0.90	0.00	291.6	0.50	453.7	0.36	607.9	0.28	649.2	0.17
15	0.90	0.00	337.5	0.45	505.2	0.25	608.0	0.16	635.3	0.09
20	0.90	0.00	388.2	0.37	545.7	0.18	619.7	0.12	678.6	0.11
25	0.90	0.00	412.7	0.34	574.4	0.15	631.9	0.09	2650.1	0.29
5	0.90	1.00	0.1	7.05	0.1	8.27	0.1	9.39	0.2	11.68
8	0.90	1.00	11.3	3.27	146.3	1.17	276.9	0.79	366.7	0.65
10	0.90	1.00	93.6	1.40	268.1	0.65	390.1	0.46	462.6	0.39
15	0.90	1.00	209.6	0.75	392.5	0.42	511.0	0.29	589.9	0.22
20	0.90	1.00	353.1	0.41	506.6	0.23	600.5	0.16	617.7	0.08
25	0.90	1.00	404.9	0.33	560.5	0.19	617.1	0.10	1751.9	0.49
15	0.65	0.00	262.7	0.55	429.2	0.35	555.1	0.28	625.8	0.21
15	0.90	0.00	337.5	0.45	505.2	0.25	608.0	0.16	625.3	0.09
15	1.05	0.00	375.4	0.38	547.2	0.22	629.6	0.14	713.9	0.12
15	0.65	1.00	208.1	0.74	378.8	0.41	484.4	0.31	568.8	0.26
15	0.90	1.00	209.6	0.75	392.5	0.42	511.0	0.29	589.9	0.22
15	1.05	1.00	215.5	0.73	400.0	0.41	512.5	0.29	587.5	0.20
10	0.90	0.50	145.8	1.01	307.9	0.53	414.8	0.45	499.8	0.41
20	0.90	0.50	375.2	0.37	523.2	0.19	609.8	0.14	638.7	0.09

ing the fragility curve for degree III from the curve for degree II.

4. RISK ASSESMENT PROCEDURE BASED ON FRAGILITY CURVES

Once the fragility curve for a specific condition is obtained, it is easy to produce the relationship between the loss and the input excitation level. The product of the loss for each damage level shown in **Table 2** and the probability of each damage level given by the fragility curve gives the estimated loss for each input excitation level as shown in **Fig. 10**, which corresponds to the **Fig. 9**. **Fig. 10** is the total of expected loss for all damage level and have already considered the variance of damage level estimation. Thus, seismic risk can be discussed without considering any more variance by **Fig. 10** if seismic hazard can be evaluated properly.

The probability of occurrence for each input excitation level can be obtained based on a seismic hazard analysis. For example, a seismic hazard analysis for Japanese coastal area was conducted based on historical earthquakes from 1885 to 1995[13]. Here, the seismic hazard for each port was examined in terms of Weibull distribution and its parameters are summarized. The expected maximum acceleration at

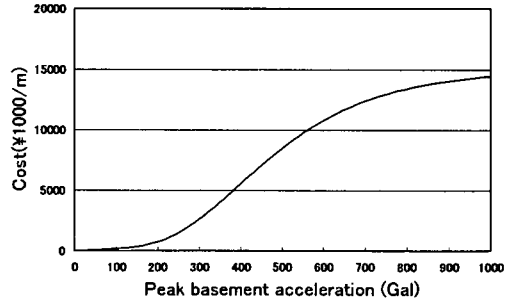

Fig.10 An example of estimated loss for each input excitation level

the basement layer in *K/N* years is evaluated as,

$$F_X(x) = 1 - \exp\left[-\left(\frac{x-B}{A}\right)^k\right] \tag{6}$$

where, x is the peak basement acceleration; $F_X(x)$ is the distribution function of x; A, B, k are the parameters for Weibull distribution; K is the period of historical earthquake records and N is the number of data points.

The return period T_R for a peak acceleration x or more is,

$$T_R = \frac{K}{N}\left(1 - F_X(x)\right)^{-1} \tag{7}$$

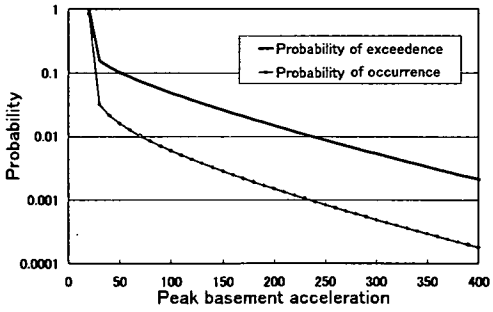

Fig.11 An example of seismic hazard evaluation

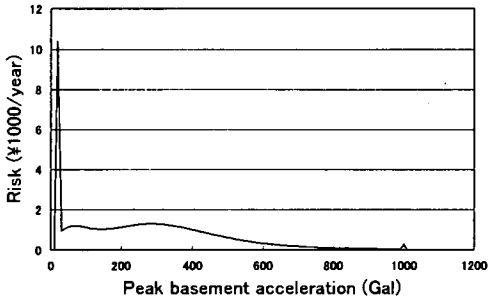

Fig. 12 An example of evaluated risk curves

Since the inverse of the return period gives the occurrence rate for a Poisson process, a rough estimation of the occurrence probability of each input acceleration level $P_h(x)$, which was discussed in equation (1), can be computed based on the results of the seismic hazard analysis mentioned above.

For example, the parameters of the Weibull distribution of SMAC equivalent acceleration at the basement layer for Sakai Port are A=51.3, B=25.8, k=0.75, K=110 and N=20. Thus the occurrence rate of peak acceleration and the seismic hazard at the base layer for Sakai Port are given as shown in **Fig.11**. Since the occurrence rate from equation (7) is given as the probability that the observed peak acceleration dose not exceeds a certain value, the hazard in equation (1), which is the annual probability of occurrence, is given by differentiating the occurrence rate.

In **Fig.11**, these curves are calculated for each 10 Gal step from 10 Gal to 1000 Gal. Since the minimum acceleration to be calculated is 25.8 Gal (corresponds to parameter B), the probability to exceed 20 Gal is given as 1.0, and the probability of occurrence for 10 Gal is 0.0. Thus the sharp change of curvature at 30 Gal is due to the numerical simplification, but it does not affect much on evaluated total risk. It should be noted here that this example did not consider the information of active faults in seismic hazard analysis. To consider active faults information properly, some modification is necessary for the evaluating procedure of occurrence rate, however, it is beyond the scope of this paper.

The SMAC equivalent acceleration is the acceleration filtered by the SMAC equivalent filter in order to get the maximum acceleration value which corresponds to the virtual acceleration, which might be observed if the SMAC-B2 type accelerograph was installed at the site[14]. Since the SMAC-B2 type accelerograph is insensitive to the high frequency component, the SMAC equivalent acceleration is less than the actual observed value. However, this difference is ignored in this paper for simplicity.

With the probability function shown in **Fig.11**, the risk curve for each fragility curve can be calculated as shown in **Fig.12**, which corresponds to **Fig.9** and **10**. The two peaks at 1000Gal and 20Gal are representing the risk for above 1000Gal and less 20Gal, respectively. Though the existence of the risk for 20Gal input sounds nonsense, it is just because the fragility curves give nonzero values even for small input acceleration. The author think it represents the damage due to inappropriate construction. The total risk (total annual expectation of loss) for a specific condition is given as the area under risk curve. This risk curve is defined as the relationship between expected loss and input level, and it is different from usual risk curve concept which was defined with occurrence probability or exceedance probability. However, proposed risk curve is easy for designer to be compared with seismic performance evaluation results which are usually expressed as a relationship between seismic damage and input level. **Table 4** shows the summary of estimated risk corresponding to **Table 3**.

5. A CASE STUDY OF SEISMIC RISK REDUCTION

Based on the parameters shown in **Table 4**, the relation between risk and seismic countermeasures can be evaluated. **Fig.13** shows the effect of geotechnical improvement on the risk. Thus, if liquefaction resistance, expressed as the equivalent SPT N values here, is improved, the risk will be reduced significantly. The effect of changing the seismic coefficient during design, which is related to the aspect ratio W/H[6], is shown in **Fig.14**. Though the seismic risk will be reduced by an increase in the seismic

Table 4 Summary of estimated seismic risk (Sakai Port case)

Equivalent SPT N values	Aspect ratio (*W/H*)	Normalized thickness of sand deposit (*D1/H*)	Estimated risk (1000yen/year)
5	0.90	0.00	41.2
8	0.90	0.00	13.8
10	0.90	0.00	9.8
15	0.90	0.00	6.3
20	0.90	0.00	3.8
25	0.90	0.00	2.2
5	0.90	1.00	10235.5
8	0.90	1.00	476.5
10	0.90	1.00	136.6
15	0.90	1.00	22.9
20	0.90	1.00	6.2
25	0.90	1.00	2.7
15	0.65	0.00	13.8
15	0.90	0.00	6.5
15	1.05	0.00	3.7
15	0.65	1.00	26.3
15	0.90	1.00	22.9
15	1.05	1.00	21.6
10	0.90	0.50	69.0
20	0.90	0.50	4.4

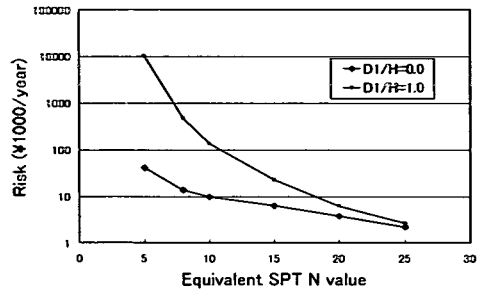

Fig.13 Effect of geotechnical improvement on the risk

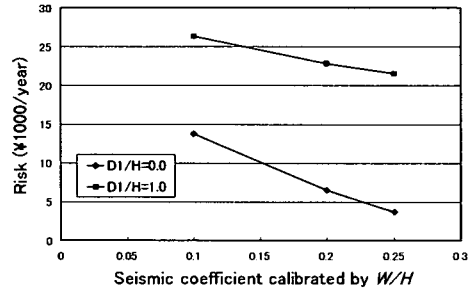

Fig.14 Effect of seismic coefficient improvement on the risk

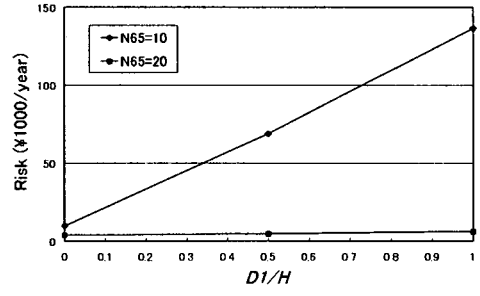

Fig.15 Effect of sand deposit thickness below the caisson

coefficient, its effect is less than that of the equivalent SPT N values. The effect of the depth of the sand deposit below the caisson is shown in **Fig.15**. For the loose deposit (*N65*=10), the risk will increase linearly with increase in depth. However, for the dense deposit (*N65*=20), the effect of the depth on the risk is negligible.

In Sakai Port, some gravity type quay walls were damaged in the 2000 Tottori-ken seibu earthquake. One of the damaged gravity type quay walls is the Showa-minami No.1 quay wall[15]. The geometric condition of the quay walls are wall height: *H*=15m, wall width: *W*=10m, and the depth of the sand deposit: *D1*=15m, as shown in **Fig.16**. Based on the equivalent SPT N values *N65*=10 as shown in **Fig.17**, the risk can be calculated in the following manner.

1) The risk for the condition that *W/H*=0.9, *D1/H*=1.0 and *N65*=10 is considered as the first estimation: approximately 136.6*1000yen/year.
2) The first estimation is corrected by the factor of the risk for the case of *W/H*=0.65, *D1/H*=1.0 (26.3*1000yen/year) and the case of *W/H*=0.9, *D1/H*=1.0 (22.9*1000yen/year): approximately 156.9*1000yen/year.

After the earthquake, the quay wall moved towards sea a maximum distance of approximately 15cm. Due to liquefaction of the backfill, sand boils and cracks with approximately 50cm wide were observed. These damage costs approximately 138,025*1000yen for the restoration of the face line length of 270m. Thus, the restoration cost per meter is approximately 511*1000yen/meter. Compared to the total risk of annual expected loss calculated above, the actual loss in this case is not so big. The author thinks the loss in this case is fortunately small compared to the total expectation of loss of the quay wall of 7,845*1000yen/meter for the operation of 50 years.

Although there are many assumptions and simplifications in the procedure described above, the estimated risk can be used as an information for the

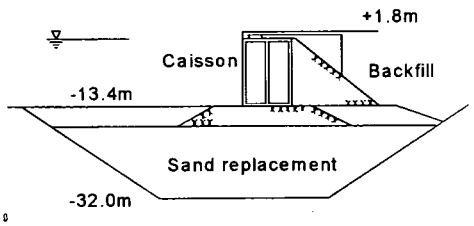

Fig.16 The cross section of the Showa-minami No.1 quay wall[15]

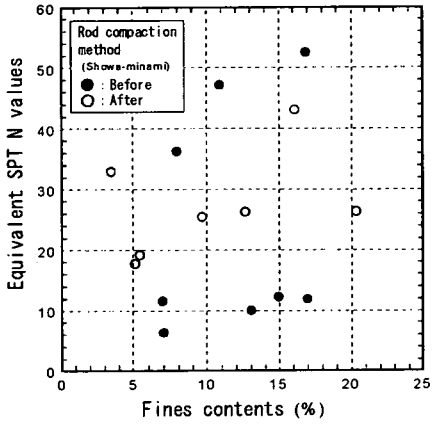

Fig.17 Geotechnical condition in the Showa-minami area[15]

damage estimation. For example, if this quay wall would be retrofitted as *N65*=25 before the earthquake, the estimated annual risk would be reduced to 3.1*1000yen (first estimation of 2.7*1000 yen with correction factor 26.3/22.9), which is approximately 1/50 of the risk before retrofit. Thus, a rough estimation of the actual loss might be 10.2*1000yen/meter, which is 1/50 of the actual loss, if the loss reduction ratio is the same as the risk reduction ratio. Actually, a quay wall with a liquefaction countermeasure in its backfill by the rod compaction method exists nearby (the Showa-minami No.2 quay wall). The equivalent SPT N values were improved to *N65*=25 in average as shown in **Fig.17**. The restoration cost for the quay wall is 19,831*1000yen for the face line of 187m (106*1000yen/m) and it was approximately 1/5 of that of the former quay wall. Since the liquefaction countermeasures were installed only in the backfill and the cross section of the quay wall is different from the former one, the loss reduction ratio is less than risk reduction ratio in this case. However, this case history indicates that the proposed risk assessment procedure can be useful information for loss mitigation of gravity type quay walls.

6. CONCLUSION

A seismic risk assessment procedure based on the fragility curve concept is proposed, and its applicability is examined with a case history in the 2000 Tottori-ken seibu earthquake. Major conclusions obtained in this paper are as follows.

1) Damage criteria for gravity type quay walls in terms of the normalized seaward displacement considering restoration cost are proposed. Though there is scatter in the restoration cost, a certain relation between the normalized seaward displacement ratio and its restoration cost is defined.
2) A procedure to generate the fragility curve for each damage level using Monte Carlo simulation is proposed. The parameter of randomness in Monte Carlo simulation is the variance of the actual displacement and the estimated displacement using a simple chart. Though two methods are proposed to consider the variance, the method considering the magnitude of estimated values showed good results.
3) The fragility curves are utilized for the risk assessment of a quay wall under a certain condition based on the result of a seismic hazard analysis. As the result of the risk assessment, the risk defined as the annual expectation of loss (*AEL*) is obtained.
4) Parameter sensitivity of the seismic risk is examined. Though increase of the thickness of the sand deposit below the caisson and decrease of the seismic coefficient increase the risk linearly, the decrease of the equivalent SPT N values behind and below the caisson increase the risk significantly.
5) The proposed risk assessment procedure is examined with a case history in the 2000 Tottori-ken seibu earthquake. Though the risk assessment procedure is based on many assumptions and simplifications, it shows that the risk defined as the annual expectation of loss (*AEL*) can be an index of seismic performance and be utilized in the decision making for seismic retrofit.

REFERENCES

1) Newmark, N. M.: Effects of earthquakes on dams and embankments, 5th Rankine lecture, *Geotechnique*, Vol.15, No.2, pp.139-160, 1965.
2) Nagao, T., Koizumi, T., Kisaka, T., Terauchi, K., Hosokawa, K., Kadowaki, Y. and Uno, K.: Evaluation of stabil-

ity of caisson type quay walls by means of present design ways and one-dimensional model analyses, *Technical note of Port and Harbour Research Institute*, No.813, pp.301-336, (in Japanese), 1995.
3) Iai, S., Ichii, K., Liu, H. and Morita, T.: Effective stress analyses of port structures, *Soils and Foundations*, Special Issue on Geotechnical Aspects of the January 17, 1995 Hyogoken-Nambu Earthquake, No.2, pp.97-114, 1998.
4) Dickenson, S.E. and Yang, D.S.: Seismically-induced deformations of caisson retaining walls in improved soils, *Geotechnical Earthquake Engineering and Soil Dynamics III*, Geotechnical Special Publication, No.75, ASCE, pp.1071-1082.
5) Uwabe, T.: Estimation of earthquake damage deformation and cost of quaywalls based on earthquake damage records, *Technical note of Port and Harbour Research Institute*, No.473, 197p., (in Japanese), 1983.
6) Ichii, K., Iai, S., Sato, Y. and Liu, H.: Seismic performance evaluation charts for gravity type quay walls, *Journal of Structural Mechanics and Earthquake Engineering*, No. 703/I-59, pp.1-11, JSCE, 2002.
7) Nakamura, T.: The Present and the Future of Seismic Risk management, *Tsuchi to Kiso*, Vol.49, No.8, Japanese Geotechnical Society, pp.1-3, (in Japanese), 2001.
8) International Navigation Association (PIANC): *Seismic design guidelines for port structures*, A.A. Balkema, p.34, 2001.
9) The Technical Committee for Earthquake Geotechnical Engineering, TC4, ISSMGE: *Case histories of post-liquefaction remediation*, Japanese geotechnical society, p.53, 2001.
10) Inatomi, T., Zen, K., Toyama, S., Uwabe, T., Iai, S., Sugano, T., Terauchi, K., Yokota, H., Fujimoto, K., Tanaka, S., Yamazaki, H., Koizumi, T., Nagao, T., Nozu, A., Miyata, M., Ichii, K., Morita, T., Minami, K., Oikawa, K., Matsunaga, Y., Ishii, M., Sugiyama, M., Takasaki, N., Kobayashi, N. and Okashita, K.: Damage to Port and Port-related Facilities by the 1995 Hyogoken-nanbu earthquake, *Technical note of the Port and Harbour Research Institute*, No. 857, (in Japanese), 1997.
11) Ueda, S., Inatomi, T., Uwabe, T., Iai, S., Kazama, M., Matsunaga, Y., Hujimoto, T., Kikuchi, Y., Miyai, S., Sekiguchi, S. and Hujimoto, Y.: Damage to Port Structures by the 1993 Kushiro-oki earthquake, *Technical note of the Port and Harbour Research Institute*, No. 766, (in Japanese), 1993.
12) Shinozuka, M., Feng, M.Q., Kim, H.K. and Kim S.H.: Nonlinear static procedure for fragility curve development, *Journal of engineering mechanics*, Vol.126, No.12, ASCE, pp.1287-1295, 2000.
13) Nozu, A., Uwabe, T., Sato, Y. and Shinozawa, T.: Relation between seismic coefficient and peak ground acceleration estimated from attenuation relations, *Technical note of Port and Harbour Research Institute*, No.893, (in Japanese), 1997.
14) Iai, S., Kurata, E. and Tsuchida, H.: Digitization and correction of strong-motion accelerograms, *Technical note of the Port and Harbour Research Institute*, No.286, (in Japanese), 1978.
15) Iai, S., Sugano, T., Yamazaki, H., Nagao, T., Nozu, A., Ichii, K., Morikawa, Y., Kohama, E., Nishimori, D., Satoh, Y., Tanaka, T., Ebihara, S., Ohmura, T. and Ohmaki, S. : Damage to Port Facilities and an airport by the 2000 Tottori-ken seibu earthquake, *Technical note of the Port and Airport Research Institute*, No. 1015, (in Japanese), 2001.

(Received January 31, 2002)

重力式岸壁の地震リスク評価法

一井康二

重力式岸壁のフラジリティカーブの考え方に基づく地震時リスク評価法を提案した．まず，重力式岸壁の被災レベル指標を地震後の復旧費用の観点に留意して無次元化した海側水平変位量により定めた．次に各々の被災レベルに対するフラジリティカーブを簡易耐震性能評価手法に基づき，モンテカルロシミュレーションにより設定する手法を提案した．そして，地震危険度解析の結果と設定したフラジリティカーブにより地震リスクを評価するものとした．また，2000年鳥取県西部地震の被災事例をもとに提案手法の適用性を検討し，耐震性強化手法の費用対効果を検討する場合の指標として，本手法による地震リスクの適用可能性を示唆した．